

# Primordial black holes and scalar induced gravitational waves from Higgs inflation with noncanonical kinetic term

Jiong Lin<sup>1,2,3,¶</sup>, Shengqing Gao<sup>3,†</sup>, Yungui Gong<sup>3,‡</sup>, Yizhou Lu<sup>3,4,§</sup>, Zhongkai Wang<sup>3,||</sup> and Fengge Zhang<sup>5,\*</sup>

<sup>1</sup>*Interdisciplinary Center for Theoretical Study, University of Science and Technology of China, Hefei, Anhui 230026, China*

<sup>2</sup>*Peng Huanwu Center for Fundamental Theory, Hefei, Anhui 230026, China*

<sup>3</sup>*School of Physics, Huazhong University of Science and Technology, Wuhan, Hubei 430074, China*

<sup>4</sup>*Department of Physics, Southern University of Science and Technology, Shenzhen 518055, China*

<sup>5</sup>*School of Physics and Astronomy, Sun Yat-sen University, Zhuhai 519088, China*



(Received 20 May 2022; accepted 31 January 2023; published 13 February 2023)

We resolve the potential-restriction problem in K/G inflation by introducing nonminimal coupling. In this context, Higgs field successfully drives inflation satisfying cosmic microwave background (CMB) observations while enhancing curvature perturbations at small scales, which in turn accounts for primordial black holes (PBHs) and scalar induced gravitational waves (SIGWs). We then uncover the effect of the noncanonical kinetic coupling function in more detail and study its observational constraint. Besides, we also give the gauge invariant expression for the integral kernel of SIGWs, which is related to terms propagating with the speed of light. Finally, the non-Gaussian effect on PBH abundance and SIGWs is studied. We find that non-Gaussianity makes PBHs form more easily, but its effect on the energy density of SIGWs is negligible.

DOI: [10.1103/PhysRevD.107.043517](https://doi.org/10.1103/PhysRevD.107.043517)

## I. INTRODUCTION

The overdense inhomogeneities in the radiation era could gravitationally collapse to form primordial black holes (PBHs) [1,2], which could be used to account for dark matter (DM) [3–11]. Due to the vast range of masses, PBHs may explain the black hole binaries with tiny effective spin detected by LIGO-Virgo Collaboration [12–15]. These density inhomogeneities can be generated from the inflationary stage, and cause collapse to form PBHs after horizon reentry. This mechanism requires the amplitude of the primordial curvature perturbation to be  $A_s \sim \mathcal{O}(10^{-2})$  [16] while the amplitude has been constrained by the cosmic microwave background (CMB) anisotropy measurements to be  $A_s \approx 2.1 \times 10^{-9}$  at the pivot scale  $k_* = 0.05 \text{ Mpc}^{-1}$  [17]. Thus the enhancement of the amplitude can occur exclusively at small scales.

A way to enhance the curvature perturbation is to provide a dramatic decrease in the velocity of the inflaton, and thus the slow-roll condition is violated. This can be achieved by

an inflationary potential with an inflection point [18–21] or a steplike feature [22]. For other enhancement mechanisms, please see Refs. [23–33]. While the inflection point does lead to the decrease in  $\dot{\phi}$ , and thus the enhancement of the power spectrum, it is a challenge to fine-tune the model parameters to enhance the power spectrum to the order of  $\mathcal{O}(10^{-2})$  with the total number of  $e$ -folds within  $N \simeq 50 - 60$  [34,35]. Meanwhile, a new mechanism with a peak function  $G(\phi)$  in the noncanonical kinetic term was proposed to enhance the primordial power spectrum at small scales [36–43]. As we will show in our paper, the peak function serves not only the enhancement of the curvature perturbation, but also the fast exit of inflation keeping the  $e$ -folds within  $N \simeq 50 - 60$ . Both sharp and broad peak functions are acceptable [38], which contribute up to  $\sim 20$   $e$ -folds so that the usual slow-roll inflation epoch should be kept to 30–40  $e$ -folds and the inflationary potential may be restricted. To cure this problem, this mechanism was improved by generalizing the noncanonical kinetic term to  $G(\phi) + f(\phi)$  [37–40]. In this paper, we will show another way to avoid this potential-restriction problem by employing the nonminimal coupling between gravity and scalar field.

On the other hand, as the only scalar field verified so far, Higgs, if drives inflation, suffers from the problem of unacceptably large tensor-to-scalar ratio  $r$ . To satisfy cosmic microwave background (CMB) observation, nonminimal (derivative) couplings  $\xi\phi^2 R$ ,  $G^{\mu\nu}\partial_\mu\phi\partial_\nu\phi$  are introduced to

\* Corresponding author.  
zhangfg5@mail.sysu.edu.cn

† gaoshengqing@hust.edu.cn

‡ ygong@hust.edu.cn

§ luyz@sustech.edu.cn

|| D202080112@hust.edu.cn

¶ jionglin@ustc.edu.cn

reduce  $r$  [44–51]. Taking into account the running of self-coupling constant and the nonminimal coupling between Higgs field and gravity, the effective potential in Einstein frame possesses an inflection point, which can enhance the curvature perturbation. However, such an enhancement is only of five orders of magnitude compared with CMB constraint  $A_s \sim \mathcal{O}(10^{-9})$ , and is unable to produce a significant abundance of PBHs [52,53]. In our paper, we will show that, by introducing a noncanonical kinetic term and a nonminimal coupling, the Higgs-field-driving inflation is compatible with CMB observation while simultaneously enhancing the curvature perturbations to order  $\mathcal{O}(10^{-2})$  at small scales.

The production of PBHs by the enhanced primordial curvature perturbation is accompanied by the generation of scalar induced gravitational waves (SIGWs) [24,54–70], for recent review, please refer [71], which consist of the stochastic background and can be tested by pulsar timing arrays (PTA) [72–75] and the space based GW observatories like Laser Interferometer Space Antenna (LISA) [76], Taiji [77] and TianQin [78]. Therefore, the observations of both PBHs and SIGWs can be used to constrain the amplitude enhancement of the primordial curvature perturbation during inflation and thus to probe the physics in the early universe.

The paper is organized as follows. In Sec. II, we show our mechanism to enhance the curvature perturbation with Higgs potential by combining the noncanonical kinetic term with the nonminimal coupling. The PBH abundance and the energy density of SIGWs generated by Higgs inflation are presented in Sec. III. In Sec. IV, we discuss the effect of the non-Gaussianity on PBH abundance and SIGWs. We conclude the paper in Sec. V.

## II. K/G INFLATION WITH NONMINIMAL COUPLING

### A. Review of K/G inflation

An idea to enhance curvature perturbation is to temporarily change the friction term in curvature perturbation equation

$$\zeta_k'' + 2\frac{z'}{z}\zeta_k' + k^2\zeta_k = 0, \quad (1)$$

into a driving term during inflation. To wit,  $z'/z < 0$ . For K/G inflation [36] with the noncanonical kinetic term  $[1 + G(\phi)]X$  where  $X = \dot{\phi}^2/2$ , the friction term is

$$\frac{z'}{z} = aH \left[ 1 + \epsilon_1 - \epsilon_2 + \frac{G_\phi \dot{\phi}}{2H(1+G)} \right], \quad (2)$$

where  $\epsilon_1 = -\dot{H}/H^2$ ,  $\epsilon_2 = -\ddot{\phi}/(H\dot{\phi})$  are slow-roll parameters. To make  $z'/z < 0$ , we could temporarily keep the second slow-roll parameter  $\epsilon_2 > 0$  and large, i.e., the

velocity of scalar field should dramatically decrease. The scalar field equation is

$$H\dot{\phi}(3 - \epsilon_2) + V_\phi^{\text{eff}} = 0, \quad (3)$$

where

$$V_\phi^{\text{eff}} = \frac{V_\phi + XG_\phi}{1 + G} \quad (4)$$

is the gradient of effective potential and the subscript  $\phi$  represents the derivative with respect to  $\phi$ . In our original paper [36], we have shown that the power spectrum can be enhanced if  $G$  has a peak. Motivated by Brans-Dicke theory [79] with coupling  $1/\phi^q$ , we choose [36,38]

$$G(\phi) = \frac{h}{1 + (|\phi - \phi_c|/c)^q}, \quad (5)$$

where  $h, c$  determine the amplitude and width of the peak, respectively.  $q$  controls the shape of the enhanced power spectrum. Larger  $q$  may give a broad peak in the power spectrum. The peak position  $\phi_c$  is related to the peak mass of PBH and the peak frequency of SIGWs. Away from the peak,  $G \approx 0$  such that the usual slow-roll inflation is recovered. In fact, by performing a field-redefinition  $d\varphi = \sqrt{1 + G(\phi)}d\phi$ , K/G inflation is equivalent to a class of the canonical inflation with the potential  $U(\varphi)$  possessing an inflection point, as shown in Fig. 1.

### B. Potential-restriction problem and K/G inflation with nonminimal coupling

Note that due to the dramatic decrease in  $\dot{\phi}$ , the peak function  $G(\phi)$  will contribute up to  $\sim 20$   $e$ -folds, and the usual slow-roll inflation epoch should be kept to  $e$ -folds

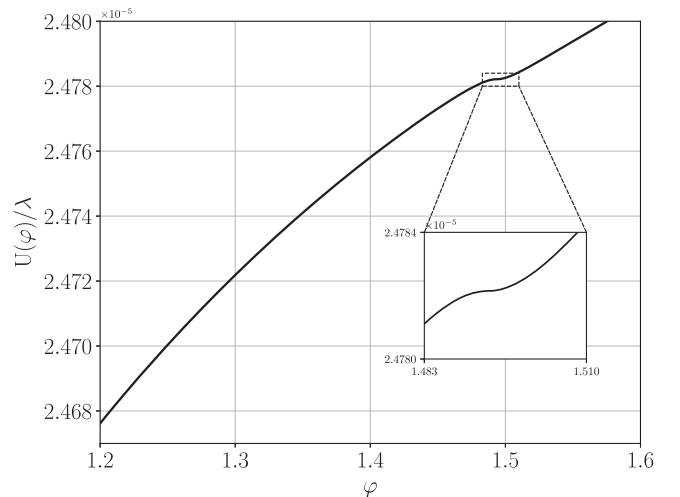


FIG. 1. After the field redefinition, the corresponding canonical potential possesses an inflection point.

TABLE I. The chosen parameters and the results for the scalar power spectrum at small peak scales.

Models	$\phi_*$	$\phi_c$	$\lambda$	$h$	$c$	$N$	$n_s$	$r$	$k_{\text{peak}}/\text{Mpc}^{-1}$	$\mathcal{P}_{\zeta(\text{peak})}$
H1	1.6	1.515	$2.3 \times 10^{-7}$	$8 \times 10^7$	$8.3 \times 10^{-11}$	63	0.97	0.0007	$2.84 \times 10^5$	0.036
H2	1.6	1.3	$2.3 \times 10^{-7}$	$8.15 \times 10^7$	$1.309 \times 10^{-10}$	63	0.966	0.0007	$4 \times 10^{12}$	0.0258
WH	1.6	1.47	$2.3 \times 10^{-7}$	$8 \times 10^7$	$7.445 \times 10^{-10}$	64	0.965	0.0007	$2.99 \times 10^5$	0.016
Q	1.3	0.98	$3.3 \times 10^{-7}$	$1.5 \times 10^7$	$9.35 \times 10^{-10}$	64	0.965	0.0007	$6.53 \times 10^{12}$	0.013

$N \simeq 30 - 40$  so that the total  $e$ -folds during inflation is within  $N \simeq 50 - 60$ . Thus the usual K/G inflation suffers from the potential-restriction problem. For power-law potential  $V = \lambda\phi^p$  with  $0 < p \leq 4$ , the  $e$ -folds during slow-roll inflation can be expressed in terms of the spectrum index as  $N_{\text{sr}} \approx (p+2)/2(1-n_s)$ . To keep  $N_{\text{sr}} \simeq 30 - 40$ , the power-law index  $p$  should be bounded by  $p \lesssim 1$ . Thus this mechanism does not work for Higgs field ( $p = 4$ ). Besides, the tensor-to-scalar ratio predicted by inflation with Higgs potential is

$$r \approx 8 \left( \frac{V_\phi}{V} \right)^2 = \frac{8p(1-n_s)}{p+2} \Big|_{p=4} \approx 0.18, \quad (6)$$

which is incompatible with observational constraints  $r_{0.05} < 0.036$  (95%CL) [80].

To realize the enhanced power spectrum with Higgs field, we combine K/G enhancement mechanism with the nonminimal coupling between Higgs field and gravity, i.e.,  $\Omega(\phi)\tilde{R}$ . The action in Jordan frame is

$$S = \int d^4x \sqrt{-\tilde{g}} \left[ \frac{1}{2} \Omega(\phi) \tilde{R}(\tilde{g}) - \frac{1}{2} \omega(\phi) \tilde{g}^{\mu\nu} \nabla_\mu \phi \nabla_\nu \phi - V(\phi) \right]. \quad (7)$$

Under conformal transformation  $g_{\mu\nu} = \Omega(\phi) \tilde{g}_{\mu\nu}$ , the action in Einstein frame becomes

$$S = \int d^4x \sqrt{-g} \left[ \frac{1}{2} R(g) - \frac{1}{2} W(\phi) g^{\mu\nu} \nabla_\mu \phi \nabla_\nu \phi - U(\phi) \right], \quad (8)$$

where

$$W(\phi) = \frac{3(d\Omega/d\phi)^2}{2\Omega^2(\phi)} + \frac{\omega(\phi)}{\Omega(\phi)}, \quad (9)$$

$$U(\phi) = V(\phi)/\Omega^2(\phi). \quad (9)$$

For power-law potential  $V(\phi) = \lambda\phi^p$ , we choose the conformal factor

$$\Omega(\phi) = 1 + \xi\phi^{p/2}. \quad (10)$$

The conformal factor can flatten the power-law potential so that the tensor-to-scalar ratio is within the CMB

observation and the  $e$ -folds of usual slow-roll inflation is kept within 30–40. By choosing the appropriate coupling function  $\omega(\phi)$  in Jordan frame, the coupling function in Einstein frame becomes

$$W(\phi) = 1 + G(\phi). \quad (11)$$

We will show now this mechanism works for generic power-law potentials. To be specific, we will numerically calculate the power spectrum for Higgs field ( $p = 4$ ) and power-law potential with  $p = 2$ . We use labels ‘‘H’’ and ‘‘WH’’ to represent Higgs inflations with the shape parameter  $q = 1$  and  $q = 6/5$ , respectively and use label ‘‘Q’’ to represent power-law inflation with  $p = 2$ . The self-coupling constant  $\lambda$  is set as  $\mathcal{O}(10^{-7})$  to satisfy the amplitude of power spectrum  $A_s \simeq 2 \times 10^{-9}$  at CMB scale. To get  $\mathcal{O}(10^{-2})$  enhancement at small scale, we choose  $h \sim \mathcal{O}(10^7)$ . The nonminimal coupling constant is taken as  $\xi = 100$ . With the model parameters listed in Table I, solving the equations for the background and the

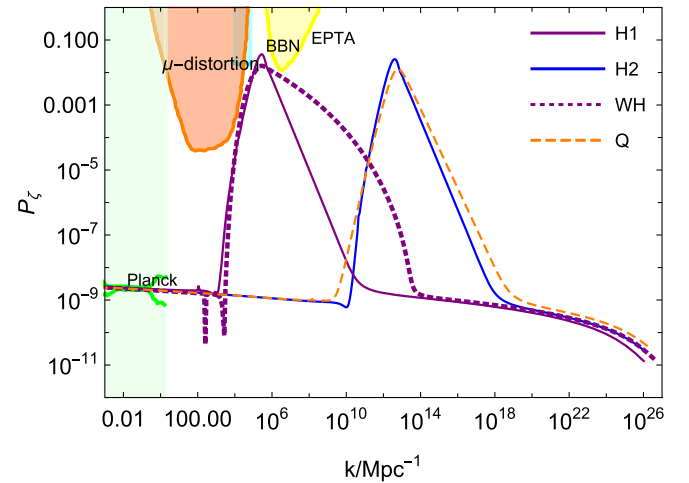


FIG. 2. The results for the scalar power spectrum for Model H1 (the purple line), Model H2 (the blue line), Model WH (the dotted purple line) and Model Q (the orange dashed line). The green lines show the scale-dependent behavior of the power spectrum. The light-green shaded region is excluded by the CMB observations [17]. The light-gray, light-blue, and thistle regions show the constraints from  $\mu$ -distortion of CMB [81], the effect on the ratio between neutron and proton during the big bang nucleosynthesis (BBN) [82] and the PTA observations [83], respectively.

perturbations numerically, the results for the scalar power spectrum are shown in Table I and Fig. 2. From these results, we can see that  $n_s$  and  $r$  are well within the CMB observation constraints,  $n_s = 0.9649 \pm 0.0042$  (68%CL) and  $r_{0.05} < 0.036$  (95%CL) [17,80]. In particular, due to conformal factor,  $r$  can be reduced to order  $\mathcal{O}(10^{-4})$ . The total  $e$ -folds are around 60. The power spectrum is enhanced to  $\mathcal{O}(10^{-2})$  at the scales  $\mathcal{O}(10^5)$  Mpc $^{-1}$  and  $\mathcal{O}(10^{12})$  Mpc $^{-1}$ . To be specific, the power spectrum for models H1 and WH are enhanced at the scale  $\mathcal{O}(10^5)$  Mpc $^{-1}$  and the power spectrum for models H2 and Q are enhanced at the scale  $\mathcal{O}(10^{12})$  Mpc $^{-1}$ . In addition, the shape parameter  $q = 1$  produces a sharp peak while the larger shape parameter  $q = 6/5$  produces the broad peak.

### C. Noncanonical kinetic coupling function and its observational constraint

In this subsection, we will uncover the effect of noncanonical kinetic coupling function in more detail and study the observational constraint on the parameter space of noncanonical kinetic coupling function.

In Fig. 3, we show the numerical results for the behaviors of the gradient of effective potential  $V_\phi^{\text{eff}}$  and the second slow-roll parameter  $\epsilon_2$  around the peak  $\phi_c = 1.515$  for Model H1. As we can see, as  $\phi$  rolls down to the right

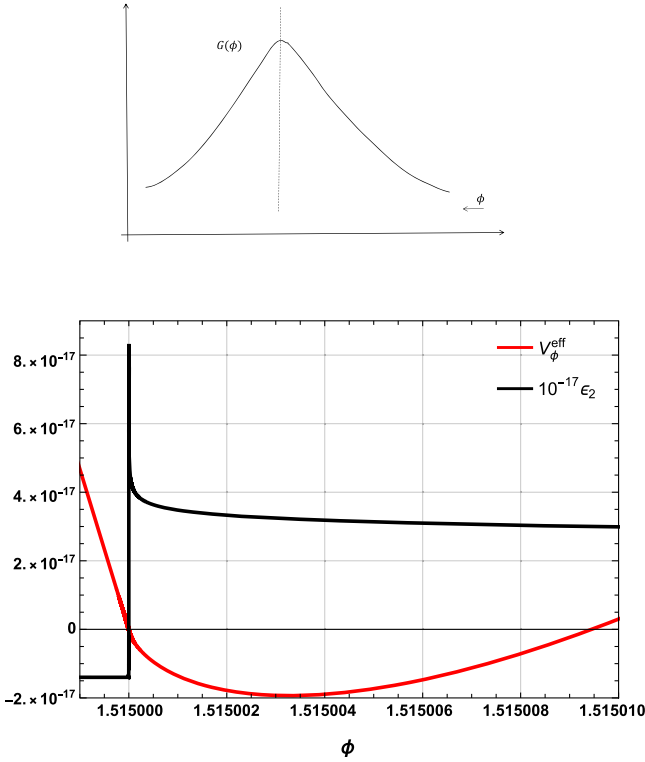


FIG. 3. The peak function  $G(\phi)$  and numerical results for the behaviors of  $V_\phi^{\text{eff}}$  and  $\epsilon_2$  around the peak  $\phi_c = 1.515$  for Model H1.

region of the peak where  $G_\phi$  is negative and very large, the gradient of effective potential satisfies  $V_\phi^{\text{eff}} < 0$  so that  $\epsilon_2 > 3$  and  $\dot{\phi}$  will dramatically decrease, and thus enhance curvature perturbation. As  $\phi$  leaves for the left region where  $G_\phi$  is positive and very large, the gradient of effective potential  $V_\phi^{\text{eff}} > 0$  such that  $\epsilon_2 < 0$ . Here  $\dot{\phi}$  will violently increase and help inflation exit. To sum up, phenomenologically, the peak function  $G$  enables not only the dramatic decrease in  $\dot{\phi}$ , which further leads to the enhancement of the curvature perturbation but also the fast exit of inflation.

The observational constraints on the present PBH abundance can be used to constrain the power spectrum for primordial curvature perturbations at small scales and thus the range of parameter space of noncanonical kinetic coupling function. Now let us study the observation constraints on K/G model with Higgs potential in detail. The LIGO merger rates [84] constrain the power spectrum as  $\mathcal{P}_\zeta \lesssim 0.04$  for  $8.9 \times 10^4$  Mpc $^{-1} \lesssim k \lesssim 4.9 \times 10^5$  Mpc $^{-1}$  [16]. This  $k$ -range of this constraint can be used to bound the amplitude parameter  $h$  of our models with the peak position  $1.5 \lesssim \phi_c$ <sup>1</sup> for the shape factor  $q = 1$  and  $1.47 \lesssim \phi_c$  for  $q = 6/5$ , which could further apply to the realizations of Models H1 and WH. To be specific, by choosing the peak position  $\phi_c = 1.515$  and  $q = 1$  and varying the width parameter  $c$ , we numerically find the upper bound on the amplitude parameter  $h$  and the results are shown in Table II. The larger the parameter  $c$  is, the lower the upper bound on  $h$  will be. This result is well comprehensive. For a wider peak function, the velocity of the inflaton decreases more dramatically. Therefore a smaller amplitude parameter  $h$  is required to realize the same enhancement on the curvature perturbation. Moreover, the white dwarf explosion [85] constrains the power spectrum to be  $\mathcal{P}_\zeta \lesssim 0.023$  for  $5.1 \times 10^{12}$  Mpc $^{-1} \lesssim k \lesssim 2 \times 10^{13}$  Mpc $^{-1}$ . This  $k$ -range of this constraint can be used to bound the amplitude parameter  $h$  of our models with the peak position  $1.27 \lesssim \phi_c$  for  $q = 1$ , which could further apply to the realizations of Models H2. The corresponding bound on  $h$  is shown in Table III and here we choose  $\phi_c = 1.28$  and  $q = 1$ .

### III. PRIMORDIAL BLACK HOLES AND SCALAR INDUCED GRAVITATIONAL WAVES

The large curvature perturbation from inflation can induce PBHs and GWs at radiation era. In this section, we will calculate PBHs abundance and SIGWs from K/G inflation with nonminimal coupling. Before that, we will first consider the gauge issue on SIGWs and give a gauge invariant expression for the integral kernel of SIGWs.

<sup>1</sup>The amplitude parameter  $h$  with a larger  $\phi_c$  is bounded by LIGO merger rates constrains, as for a larger  $\phi_c$ , one could always choose a larger  $h$  so that the corresponding peak scale locates within the scale where LIGO merger rates constrain.

TABLE II. Constraint on K/G model with Higgs potential from LIGO merger rate. Here  $\phi_c = 1.515$  and  $q = 1$ .

$c$	$8.3 \times 10^{-11}$	$8.8 \times 10^{-11}$	$9.3 \times 10^{-11}$	$1 \times 10^{-10}$	$2 \times 10^{-10}$
Upper bound on $h$	$8.05 \times 10^7$	$7.6 \times 10^7$	$7.2 \times 10^7$	$6.7 \times 10^7$	$3.4 \times 10^7$

 TABLE III. Constraint on K/G model with Higgs potential from white dwarf explosion. Here  $\phi_c = 1.28$  and  $q = 1$ .

$c$	$1.4 \times 10^{-10}$	$2 \times 10^{-10}$	$2.5 \times 10^{-10}$	$3 \times 10^{-10}$	$3.2 \times 10^{-10}$
Upper bound on $h$	$8 \times 10^7$	$5.65 \times 10^7$	$4.55 \times 10^7$	$3.85 \times 10^7$	$3.7 \times 10^7$

### A. The gauge invariant expression for the integral kernel of SIGWs

Considering a metric perturbation

$$ds^2 = a^2 \left[ -(1 + 2\phi)d\tau^2 + 2B_{,i}dx^i d\tau + \left( (1 - 2\psi)\delta_{ij} + 2E_{,ij} + \frac{1}{2}h_{ij}^{\text{TT}} \right) dx^i dx^j \right], \quad (12)$$

the scalar-induced tensor perturbations  $h_{ij}^{\text{TT}}$  satisfy [56,57]

$$h_{ij}^{\text{TT}''} + 2\mathcal{H}h_{ij}^{\text{TT}'} - \nabla^2 h_{ij}^{\text{TT}} = 4T_{ij}^{lm} s_{lm}, \quad (13)$$

where  $\mathcal{H} = aH$ ,  $T_{ij}^{lm}$  is the projection tensor extracting the transverse and traceless part of a tensor and the scalar source is [86]

$$\begin{aligned} -s_{ij} = & \psi_{,i}\psi_{,j} + \phi_{,i}\phi_{,j} - \sigma_{,ij}(\phi' + \psi' - \nabla^2\sigma) + (\psi'_{,i}\sigma_{,j} + \psi'_{,j}\sigma_{,i}) - \sigma_{,ik}\sigma_{,jk} + 2\psi_{,ij}(\phi + \psi) \\ & - 8\pi G a^2(\rho_0 + P_0)\delta V_{,i}\delta V_{,j} - 2\psi_{,ij}\nabla^2 E + 2E_{,ij}(\psi'' + 2\mathcal{H}\psi' - \nabla^2\psi) - E'_{,ik}E'_{,jk} \\ & + E_{,ikl}E_{,jkl} + 2(\psi_{,jk}E_{,ik} + \psi_{,ik}E_{,jk}) - 2\mathcal{H}(\psi_{,i}E'_{,j} + \psi_{,j}E'_{,i}) - (\psi'_{,i}E'_{,j} + \psi'_{,j}E'_{,i}) \\ & - (\psi_{,i}E''_{,j} + \psi_{,j}E''_{,i}) + 2E'_{,ij}\psi' + E_{,ijk}(E'' + 2\mathcal{H}E' - \nabla^2 E)_{,k}, \end{aligned} \quad (14)$$

where  $\sigma = E' - B$  is the shear potential. Solving Eq. (13), the current energy density of SIGWs can be expressed as [66,87]

$$\Omega_{\text{GW}}(k, \eta_0) = \frac{1}{6} \frac{\Omega_r(\eta_0)}{\Omega_r(\eta)} \left( \frac{k}{aH} \right)^2 \int_0^\infty dv \int_{|1-v|}^{1+v} du \left\{ \left[ \frac{4v^2 - (1 - u^2 + v^2)^2}{4uv} \right]^2 \frac{I_{\text{RD}}^2(u, v, x \rightarrow \infty) \mathcal{P}_\zeta(kv) \mathcal{P}_\zeta(ku)}{I_{\text{RD}}^2(u, v, x \rightarrow \infty)} \right\}, \quad (15)$$

where  $u = |\mathbf{k} - \tilde{\mathbf{k}}|/k$ ,  $v = \tilde{k}/k$ ,  $x = k\tau$ ,  $\Omega_r$  is the fraction energy density of radiation, the overbar denotes the oscillation time average and  $I_{\text{RD}}$  is the integral kernel in radiation domination. In Newtonian gauge, the integral kernel is

$$\begin{aligned} I_{\text{N}}(u, v, x) = & \int_1^x dy y \sin(x - y) \{ 3T_{\text{N}}(uy)T_{\text{N}}(vy) \\ & + y[T_{\text{N}}(vy)uT'_{\text{N}}(uy) + vT'_{\text{N}}(vy)T_{\text{N}}(uy)] \\ & + y^2 uv T'_{\text{N}}(uy)T'_{\text{N}}(vy) \}, \end{aligned} \quad (16)$$

where the transfer function  $T_{\text{N}}$  in the radiation domination is

$$T_{\text{N}}(x) = \frac{9}{x^2} \left( \frac{\sin(x/\sqrt{3})}{x/\sqrt{3}} - \cos(x/\sqrt{3}) \right). \quad (17)$$

The analytical expression for  $I_{\text{RD}}$  in Newtonian gauge was given in Refs. [87–89]. However, SIGWs suffer from the gauge issue [86,90–98]. On one hand, this issue may be related to the definitions of gravitational waves and their energy [98]. On the other hand, as noted in Refs. [92,94], only terms that oscillate as  $\sin x$  and  $\cos x$  propagate with the speed of light. They are taken as genuine GWs out of second-order tensor perturbations. Now let us write down the integral kernel in arbitrary gauge and extract the terms that propagate with speed of light. The integral kernel in arbitrary gauge can be obtained by the transformation

$$I_{\text{N}}(u, v, x) \rightarrow I_{\text{N}}(u, v, x) + I_{\chi}(u, v, x), \quad (18)$$

where



$$\begin{aligned}
 I_\chi(u, v, x) = & -\frac{1}{4uv} \left( \frac{3+3w}{5+3w} \right)^2 \left[ -4 \left( \frac{u}{v} T_N(ux) T_\beta(vx) + \frac{v}{u} T_N(vx) T_\beta(ux) \right) \right. \\
 & + 2T_\alpha(ux) T_\alpha(vx) + 4 \frac{\mathcal{H}}{k} \left( \frac{1}{v} T_\alpha(ux) T_\beta(vx) + \frac{1}{u} T_\beta(ux) T_\alpha(vx) \right) \\
 & \left. + \frac{1-u^2-v^2}{uv} T_\beta(ux) T_\beta(vx) \right], \tag{19}
 \end{aligned}$$

$T_\alpha, T_\beta$  are related to gauge transformation. Note that the gauge transformation can be expressed in terms of scalar perturbations, thus  $I_\chi$  only contains terms with sound speed  $c_s^2 = w$  instead of the speed of light. Omitting terms that do not propagate with speed of light, the kernel of genuine SIGWs (the terms of  $\sin x$  and  $\cos x$ , which propagate with the speed of light) in arbitrary gauge is<sup>2</sup>

$$\begin{aligned}
 I_{\text{GW}}(u, v, x) = & \frac{3}{4u^3v^3x} \left\{ -4uv(u^2 + v^2 - 3) \sin x + (u^2 + v^2 - 3)^2 \right. \\
 & \times \left[ \sin x \left( \text{Ci} \left[ \left( 1 + \frac{u-v}{\sqrt{3}} \right) x \right] + \text{Ci} \left[ \left( 1 + \frac{v-u}{\sqrt{3}} \right) x \right] - \text{Ci} \left[ \left( 1 + \frac{u+v}{\sqrt{3}} \right) x \right] \right. \right. \\
 & - \text{Ci} \left[ \left| 1 - \frac{u+v}{\sqrt{3}} \right| x \right] + \log \left| \frac{3-(u+v)^2}{3-(u-v)^2} \right| \left. \right) + \cos x \left( -\text{Si} \left[ \left( 1 + \frac{u-v}{\sqrt{3}} \right) x \right] \right. \\
 & \left. \left. - \text{Si} \left[ \left( 1 + \frac{v-u}{\sqrt{3}} \right) x \right] + \text{Si} \left[ \left( 1 - \frac{u+v}{\sqrt{3}} \right) x \right] + \text{Si} \left[ \left( 1 + \frac{u+v}{\sqrt{3}} \right) x \right] \right) \right] \left. \right\}, \tag{20}
 \end{aligned}$$

where

$$\text{Si}(x) \equiv \int_0^x \frac{\sin y}{y} dy, \quad \text{Ci}(x) \equiv - \int_x^\infty \frac{\cos y}{y} dy. \tag{21}$$

At late time  $x \rightarrow \infty$ , the integral kernel of genuine SIGWs becomes

$$\begin{aligned}
 \overline{I_{\text{GW}}^2}(u, v, x \rightarrow \infty) = & \overline{I_{\text{N}}^2}(u, v, x \rightarrow \infty) \\
 = & \frac{1}{2x^2} \left( \frac{3(u^2 + v^2 - 3)}{4u^3v^3} \right)^2 \left\{ \left( -4uv + (u^2 + v^2 - 3) \log \left| \frac{3-(u+v)^2}{3-(u-v)^2} \right| \right)^2 \right. \\
 & \left. + \pi^2 (u^2 + v^2 - 3)^2 \Theta(u + v - \sqrt{3}) \right\}, \tag{22}
 \end{aligned}$$

where the Heaviside theta function

$$\Theta(x) = \begin{cases} 1, & x \geq 0 \\ 0, & x < 0 \end{cases}. \tag{23}$$

## B. PBHs and SIGWs from Higgs inflation

The overdense region would gravitationally collapse to form PBHs when horizon reentry during radiation dominated era. The current fractional energy density of PBHs with mass  $M$  to DM is [8,20]

$$\begin{aligned}
 Y_{\text{PBH}}(M) = & \frac{\beta(M)}{3.94 \times 10^{-9}} \left( \frac{\gamma}{0.2} \right)^{1/2} \left( \frac{g_*}{107.5} \right)^{-1/4} \\
 & \times \left( \frac{0.12}{\Omega_{\text{DM}} h^2} \right) \left( \frac{M}{M_\odot} \right)^{-1/2}, \tag{24}
 \end{aligned}$$

where  $M_\odot$  is the solar mass,  $\gamma = 0.2$  [99].  $g_*$  is the effective degrees of freedom at the formation time. For the temperature  $T > 300$  GeV,  $g_* = 107.5$  and for  $0.5$  MeV  $< T < 300$  GeV,  $g_* = 10.75$ .  $\Omega_{\text{DM}}$  is the current energy density parameter of DM and we take  $\Omega_{\text{DM}} h^2 = 0.12$  [100]. The PBH mass  $M$  is related to the scale  $k$  as [20]

$$M(k) = 3.68 \left( \frac{\gamma}{0.2} \right) \left( \frac{g_*}{107.5} \right)^{-1/6} \left( \frac{k}{10^6 \text{ Mpc}^{-1}} \right)^{-2} M_\odot. \tag{25}$$

<sup>2</sup>This is the solution with the lower limit being 0 in (16). In fact, according to Ref. [89], the difference can usually be ignored.

TABLE IV. The results for PBH abundance and critical frequency of SIGWs.

Model	$k_{\text{peak}}/\text{Mpc}^{-1}$	$\mathcal{P}_\zeta(\text{peak})$	$M_{\text{PBH}}^{\text{peak}}/M_\odot$	$Y_{\text{PBH}}^G(\text{peak})$	$f_c/\text{Hz}$
H1	$2.84 \times 10^5$	0.036	29	$5.3 \times 10^{-4}$	$4.8 \times 10^{-10}$
H2	$4 \times 10^{12}$	0.0258	$1.48 \times 10^{-13}$	0.88	$6.8 \times 10^{-3}$
WH	$2.99 \times 10^5$	0.016			$5 \times 10^{-10}$
Q	$6.53 \times 10^{12}$	0.013			$1.1 \times 10^{-2}$

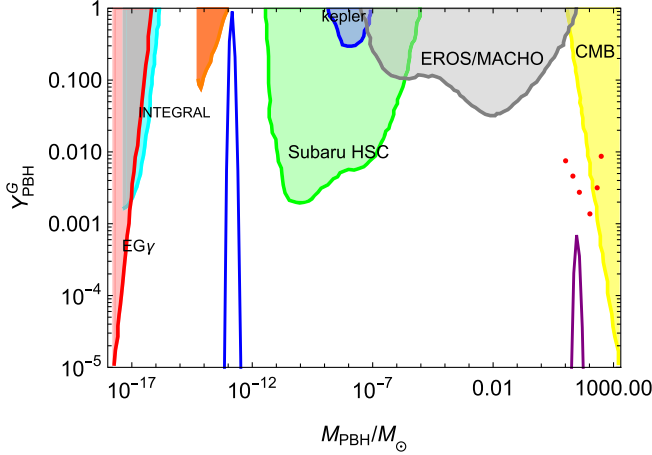


FIG. 4. The PBH abundances for Model H1 (the purple line) and Model H2 (the blue line) using the Gaussian formulate  $\beta^G$  for the fraction energy density of PBHs at the formation. The shaded regions show the observational constraints on the PBH abundance: the red region from extragalactic gamma-rays by PBH evaporation (EG $\gamma$ ) [114], the cyan region from galactic center 511 keV gamma-ray line (INTEGRAL) [115,116], the orange region from white dwarf explosion (WD) [85], the green region from microlensing events with Subaru HSC [117], the blue region from the Kepler satellite [118], the gray region from the EROS/MACHO [119], the red points from LIGO merger rate [84] and the yellow region from accretion constraints by CMB [120,121].

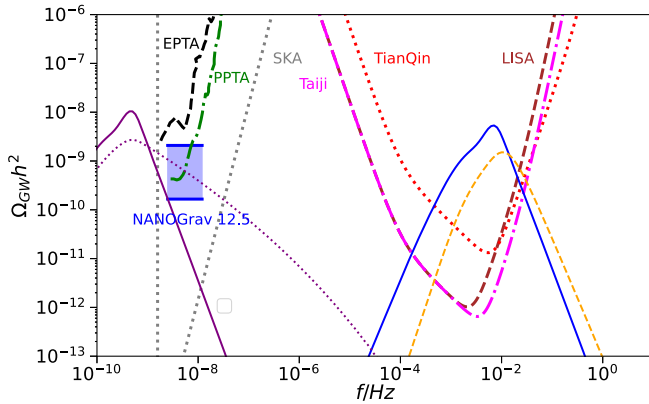


FIG. 5. The SIGWs from Model H1 (the purple line), Model H2 (the blue line), WH (the purple dotted line), and Q (the orange dashed line). The black dashed curve shows the EPTA limit [72–75], the gray dotted curve denotes the SKA limit [122], the brown dashed curve shows the LISA limit [76], the red dot-dashed curve denotes the TianQin limit [78] and the dotted magenta curve denotes the TaiJi limit [77].

$\beta(M)$  is the fractional energy density of PBHs at the formation. For Gaussian comoving curvature perturbation  $\zeta$  [101,102], we have

$$\beta^G(M) \approx \sqrt{\frac{2}{\pi}} \frac{\sqrt{\mathcal{P}_\zeta}}{\mu_c} \exp\left(-\frac{\mu_c^2}{2\mathcal{P}_\zeta}\right), \quad (26)$$

where  $\delta_c$  is the threshold for the PBH formation and  $\mu_c = 9\sqrt{2}\delta_c/4$  [38]. Here we choose  $\delta_c = 0.4$  [102–106] for calculations.

Substituting the obtained power spectrum from Higgs inflation in Sec. II B into Eqs. (24) and (15), we get the PBH abundances<sup>3</sup> as shown in Table IV and Fig. 4 and the current energy densities of SIGWs as shown in Fig. 5. Model H1 produces PBHs with mass  $M \simeq 30M_\odot$  and the abundance  $Y^{\text{peak}} \simeq 5.3 \times 10^{-4}$ , which may explain the BH event GW150914 observed by LIGO [12]. The accompanying SIGWs have the peak frequency  $f \sim 4.8 \times 10^{-10}$  Hz and could be tested by SKA. Although Model WH cannot produce significant PBHs using the Gaussian formulate Eq. (26), the energy density of SIGWs lies within the  $2\sigma$  region of the NANOGrav signal [107–113]. Thus NANOGrav signal may originate from the Higgs field. Models H2 produces PBHs with mass  $M \simeq \mathcal{O}(10^{-13})M_\odot$ . In these mass ranges, PBHs can constitute almost all DM. The accompanying SIGWs has the millihertz frequency, which can be tested by future space-based detectors like LISA, TaiJi, and TianQin.

#### IV. PRIMORDIAL NON-GAUSSIANITY

Due to the violation of the slow-roll condition, the non-Gaussianity may be large. Thus it is necessary to investigate the impact of non-Gaussianity on PBH abundance and SIGWs. In this section, we first compute the primordial non-Gaussianity from our model and then we discuss its effects on PBH abundance and the energy density of SIGWs.

The non-Gaussianity parameter  $f_{\text{NL}}$  is [123]

$$f_{\text{NL}}(k_1, k_2, k_3) = \frac{5}{6} \frac{B_\zeta(k_1, k_2, k_3)}{P_\zeta(k_1)P_\zeta(k_2) + P_\zeta(k_2)P_\zeta(k_3) + P_\zeta(k_3)P_\zeta(k_1)}, \quad (27)$$

<sup>3</sup>Here we use the Gaussian formulate Eq. (26) for the fraction energy density of PBHs at the formation. In the next section, the non-Gaussianity effect will be taken into account.

where  $P_\zeta(k) = 2\pi^2 \mathcal{P}_\zeta(k)/k^3$  and the bispectrum is defined as

$$\langle \hat{\zeta}_{k_1} \hat{\zeta}_{k_2} \hat{\zeta}_{k_3} \rangle = (2\pi)^3 \delta^3(\mathbf{k}_1 + \mathbf{k}_2 + \mathbf{k}_3) B_\zeta(k_1, k_2, k_3). \quad (28)$$

The expression for the bispectrum is presented in the Appendix.

With the parameter sets in Table I, we numerically compute the non-Gaussianity parameter  $f_{\text{NL}}$  and the results are shown in Figs. 6 and 7. For single-field inflation, there is a consistency relation [124,125] that relates the bispectrum and power spectrum,

$$\lim_{k_3 \rightarrow 0} f_{\text{NL}}(k_1, k_2, k_3) = \frac{5}{12}(1 - n_s), \quad \text{for } k_1 = k_2, \quad (29)$$

which can be used to test our numerical computation of non-Gaussianity. From Figs. 6 and 7, we can see that the spectrum index  $n_s - 1$  matches with  $-12f_{\text{NL}}/5$  in squeezed limit. Note that from the expressions for bispectrum Eqs. (A5) and (A8), the large non-Gaussianity parameter

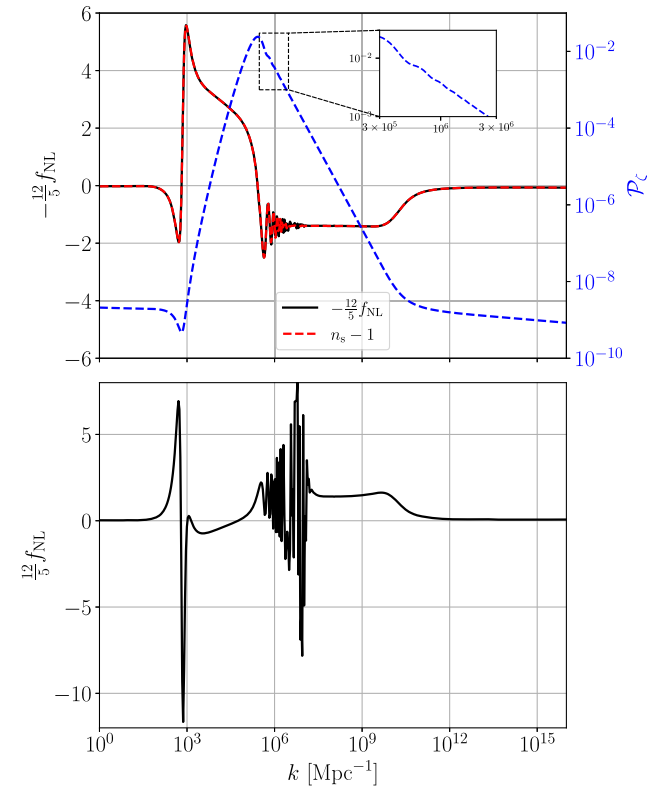


FIG. 6. The power spectrum of primordial curvature perturbation and the non-Gaussianity parameter  $f_{\text{NL}}$  for the model H1. We show the power spectrum with the blue dashed line,  $-12f_{\text{NL}}/5$  in the squeezed limit with the solid black line for the modes  $k_1 = k_2 = 10^6 k_3 = k$  and the scalar spectral tilt  $n_s - 1$  with the red dashed line in the upper panel. The insets show the oscillations in  $\mathcal{P}_\zeta$ . The lower panel shows  $12f_{\text{NL}}/5$  in the equilateral limit for the modes  $k_1 = k_2 = k_3 = k$ .

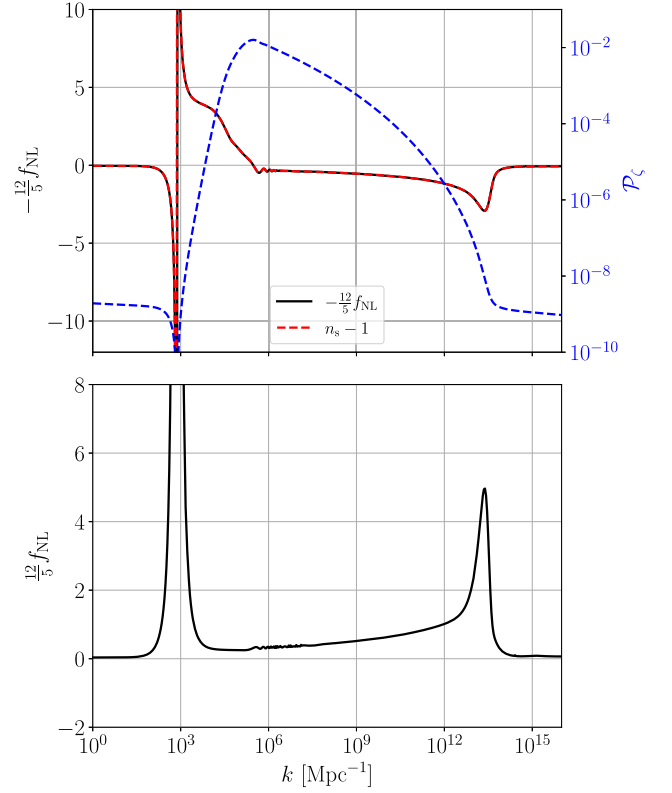


FIG. 7. The power spectrum of primordial curvature perturbation and the non-Gaussianity parameter  $f_{\text{NL}}$  for the model WH. We show  $-12f_{\text{NL}}/5$  in the squeezed limit with the solid black line for the modes  $k_1 = k_2 = 10^6 k_3 = k$  and  $12f_{\text{NL}}/5$  in the equilateral limit for the modes  $k_1 = k_2 = k_3 = k$  in the upper and lower panels, respectively. We also show the power spectrum with the blue dashed line and the scalar spectral tilt  $n_s - 1$  with the red dashed line in the upper panel.

$f_{\text{NL}}$  may originate from the dramatic change in the velocity and acceleration of the inflaton. Note that the second slow-roll parameter  $\epsilon_2$  for H1 ( $q = 1$ , sharp power spectrum) changes more dramatically than WH ( $q = 6/5$ , broad power spectrum) around the peak scale. Thus the non-Gaussianity parameter of WH around the peak region always stays smaller than H1, as shown in Table V.

### A. Non-Gaussian effect on PBH abundance

Now let us consider the non-Gaussian effect on PBH abundance. Taking the non-Gaussianity correction into account, the fraction energy density of PBH at the formation becomes [126–129]

TABLE V. The results for the non-Gaussianity parameter  $f_{\text{NL}}$  and the third cumulant  $\Delta_3$ .

Model	$f_{\text{NL}}(k_{\text{peak}}, k_{\text{peak}}, k_{\text{peak}})$	$\Delta_3$
H1	0.62	25
H2	0.53	30
WH	0.13	12



$$\beta = e^{\Delta_3} \beta^G. \quad (30)$$

The mass of PBHs we consider is almost monochromatic, thus the third cumulant  $\Delta_3$  can be approximately expressed as [42]<sup>4</sup>

$$\Delta_3 \approx 23 \frac{\delta_c^3}{\mathcal{P}_\zeta(k_{\text{peak}})} f_{\text{NL}}(k_{\text{peak}}, k_{\text{peak}}, k_{\text{peak}}). \quad (31)$$

In Table V, we show the results for the non-Gaussianity parameter  $f_{\text{NL}}$  and the third cumulant  $\Delta_3$ . The non-Gaussianity parameter  $f_{\text{NL}}$  is of order  $\mathcal{O}(10^{-1})$ . In fact, during inflation with the sharper peak, the velocity of the inflaton changes more dramatically such that the non-Gaussianity effect is more significant than inflation with the broad peak. The non-Gaussianity correction has a significant enhancement on PBH abundance, which means the formation of PBHs is easier with the consideration of the non-Gaussianity. The PBH abundance is underestimated with Gaussian statistics. Note that in Ref. [41], we have used the approximation formula for non-Gaussian PBH abundance proposed in Ref. [130] and concluded that for K/G inflation, the non-Gaussian effect on PBH abundance can be neglected due to  $J_{\text{peak}} \sim \mathcal{O}(10^{-3}) \ll 1$ . However, this analysis neglected the factor before  $J_{\text{peak}}$ , i.e.,  $(\hat{\zeta}^5 - 8\hat{\zeta}^3 + 9\hat{\zeta})J_{\text{peak}}$ , where  $\hat{\zeta} \equiv \zeta/\sqrt{\mathcal{P}_\zeta(k_{\text{peak}})}$  and  $J \equiv \langle \zeta_{RM}^3 \rangle_c / \sigma_{RM}^3 / 6$ . Taking the critical value  $\zeta_c \sim \mathcal{O}(1)$  [19,103,104,126,131] and thus  $\hat{\zeta}_c \sim \mathcal{O}(10)$ , then we can find  $(\hat{\zeta}_c^5 - 8\hat{\zeta}_c^3 + 9\hat{\zeta}_c)J_{\text{peak}} \sim \mathcal{O}(10^2)$ , which is large enough so that the non-Gaussian effect on PBH cannot be neglected. On the other hand, note that the formula for non-Gaussian PBH abundance in Ref. [130] is an approximation result requiring the term (prefactor  $\times J$ )  $\ll 1$ , which is not satisfied in K/G inflation. Thus in this paper and Ref. [42], we adopt the exact formula for non-Gaussian PBH abundance proposed in Ref. [126].

### B. Non-Gaussian effect on SIGW

To investigate the non-Gaussian effect on SIGWs, we first consider the power spectrum with the non-Gaussian correction. The comoving curvature perturbation with the nonlinear corrections can be expressed as [132,133]

$$\zeta(\mathbf{x}) = \zeta^G(\mathbf{x}) + \frac{3}{5} f_{\text{NL}} (\zeta^G(\mathbf{x})^2 - \langle \zeta^G(\mathbf{x})^2 \rangle), \quad (32)$$

where  $\zeta^G$  is the Gaussian part of the curvature perturbation. Thus the power spectrum is

$$\mathcal{P}_\zeta(k) = \mathcal{P}_\zeta^G(k) + \mathcal{P}_\zeta^{\text{NG}}(k), \quad (33)$$

with the non-Gaussian correction of the power spectrum

$$\mathcal{P}_\zeta^{\text{NG}}(k) = \left(\frac{3}{5}\right)^2 \frac{k^3}{2\pi} f_{\text{NL}}^2 \int d^3\mathbf{p} \frac{\mathcal{P}_\zeta^G(p)}{p^3} \frac{\mathcal{P}_\zeta^G(|\mathbf{k}-\mathbf{p}|)}{|\mathbf{k}-\mathbf{p}|^3}. \quad (34)$$

For our model with  $f_{\text{NL}} \sim \mathcal{O}(10^{-1})$  at peak scales, we have  $\mathcal{P}_\zeta^{\text{NG}}(k) \ll \mathcal{P}_\zeta^G(k)$  and thus the non-Gaussian effect can be neglected when calculating SIGWs.

## V. CONCLUSIONS

K/G inflation with a noncanonical kinetic term  $(1 + G(\phi))X$  can produce enhanced curvature perturbations at small scales if the coupling function  $G(\phi)$  has a peak. However, due to the dramatic decrease in  $\dot{\phi}$ , the peak function  $G(\phi)$  will contribute up to  $\sim 20$   $e$ -folds and the usual slow-roll inflation epoch endures around 30–40  $e$ -folds. For power-law potential  $V = \lambda\phi^p$ , this indicates  $p$  should be bounded as  $p \lesssim 1$ . In particular, this mechanism does not work for Higgs potential  $V = \lambda\phi^4$ . To resolve potential-restriction problem and produce PBHs and SIGWs in Higgs inflation, we introduce K/G inflation with nonminimal coupling and show that the curvature perturbation at small scales can be enhanced by the Higgs field while satisfying the constraints from CMB observations. To be specific, in the Einstein frame, the conformal factor flattens the Higgs potential such that the  $e$ -folds during slow-roll inflation are within 40 and the tensor-to-scalar ratio is reduced.

We then study the noncanonical kinetic coupling function in detail. On the one hand, phenomenologically, we find that the noncanonical kinetic coupling function not only drives the dramatic decreases in  $\dot{\phi}$  and thus the enhancement of the curvature perturbation but also helps the exit of inflation. On the other hand, we study the observational constraints from LIGO merger rates and the white dwarf explosion on the parameter space of the noncanonical kinetic coupling function. Our numerical results show that for a given width parameter  $c$ , there is an upper bound on the amplitude parameter  $h$  and as  $c$  gets larger, the upper bound on  $h$  decreases. The reason is that the larger  $c$  indicates a wider peak function and thus the velocity of the inflaton decreases more dramatically and a smaller amplitude parameter  $h$  is required to realize the same enhancement on curvature perturbations.

By varying the peak position, the curvature perturbation can be enhanced at different scales and thus different mass ranges of PBHs and frequencies of SIGWs can be produced. PBHs with mass  $\mathcal{O}(10)M_\odot$ ,  $\mathcal{O}(10^{-12})M_\odot$  from models H1 and H2 may explain BHs in LIGO-Virgo events and almost all the DM, respectively. For SIGWs, we give the gauge invariant expression for the integral kernel of genuine SIGWs, which is related to terms propagating with the speed of light. The energy density of SIGWs from the model WH lies within the  $2\sigma$  region of the NANOGrav signal. Thus NANOGrav signal may originate from the Higgs field. SIGWs from the model H2 have the millihertz frequency, which can be tested by future space-based detectors like LISA, TaiJi, and TianQin.

<sup>4</sup>The sign of  $\Delta_3$  differs from that in [42], which is incorrect. See the erratum of [42].

Due to the violation of the slow-roll condition, the non-Gaussianity may have a significant effect on PBH abundance and SIGWs. Around the peak scale, we find that the non-Gaussianity parameter  $f_{\text{NL}}$  of sharp power spectrum is larger than that of broad power spectrum due to more dramatic change in the velocity of the inflaton. For our models, the non-Gaussianity parameter  $f_{\text{NL}}$  in the equilateral limit is of order  $\mathcal{O}(10^{-1})$  at peak scales and the non-Gaussianity correction has a significant enhancement on PBH abundance. Notwithstanding, the energy density of SIGWs remains invariant even if we take the non-Gaussianity into account, as the power spectrum receives very tiny corrections.

## ACKNOWLEDGMENTS

This research is supported in part by the National Natural Science Foundation of China under Grant No. 11875136, and the Major Program of the National Natural Science Foundation of China under Grant No. 11690021. J.L. is also supported by the National Natural Science Foundation of China under Grants No. 12247103, No. 12047502 and No. 12247117. Y.L. is also supported by the China Postdoctoral Science Foundation under Grant No. 2022TQ0140.

## APPENDIX: THE EXPRESSION FOR THE BISPECTRUM

The bispectrum  $B_\zeta(k_1, k_2, k_3)$  is [134–136]

$$B_\zeta(k_1, k_2, k_3) = \sum_{i=1}^{10} B_\zeta^i(k_1, k_2, k_3), \quad (\text{A1})$$

$$B_\zeta^1(k_1, k_2, k_3) = -4\text{Im} \left[ \zeta_{k_1}(\tau_*) \zeta_{k_2}(\tau_*) \zeta_{k_3}(\tau_*) \int_{\tau_i}^{\tau_*} d\tau a^2 \epsilon_1^2 \{ \zeta_{k_1}^*(\tau) \zeta_{k_2}^{\prime*}(\tau) \zeta_{k_3}^{\prime*}(\tau) + \text{perm} \} \right], \quad (\text{A2})$$

$$B_\zeta^2(k_1, k_2, k_3) = 2\text{Im} \left[ \zeta_{k_1}(\tau_*) \zeta_{k_2}(\tau_*) \zeta_{k_3}(\tau_*) \int_{\tau_i}^{\tau_*} d\tau a^2 \epsilon_1^2 \{ (k_1^2 - k_2^2 - k_3^2) \zeta_{k_1}^*(\tau) \zeta_{k_2}^*(\tau) \zeta_{k_3}^*(\tau) + \text{perm} \} \right], \quad (\text{A3})$$

$$B_\zeta^3(k_1, k_2, k_3) = 2\text{Im} \left[ \zeta_{k_1}(\tau_*) \zeta_{k_2}(\tau_*) \zeta_{k_3}(\tau_*) \int_{\tau_i}^{\tau_*} d\tau a^2 \epsilon_1^2 \left\{ \left( \frac{k_2^2 - k_1^2 - k_3^2}{k_1^2} + \frac{k_1^2 - k_2^2 - k_3^2}{k_2^2} \right) \zeta_{k_1}^{\prime*}(\tau) \zeta_{k_2}^{\prime*}(\tau) \zeta_{k_3}^*(\tau) + \text{perm} \right\} \right], \quad (\text{A4})$$

$$B_\zeta^4(k_1, k_2, k_3) = -2\text{Im} \left[ \zeta_{k_1}(\tau_*) \zeta_{k_2}(\tau_*) \zeta_{k_3}(\tau_*) \int_{\tau_i}^{\tau_*} d\tau a^2 \epsilon_1 \eta' \{ \zeta_{k_1}^*(\tau) \zeta_{k_2}^{\prime*}(\tau) \zeta_{k_3}^{\prime*}(\tau) + \text{perm} \} \right], \quad (\text{A5})$$

$$B_\zeta^5(k_1, k_2, k_3) = -\frac{1}{2} \text{Im} \left[ \zeta_{k_1}(\tau_*) \zeta_{k_2}(\tau_*) \zeta_{k_3}(\tau_*) \int_{\tau_i}^{\tau_*} d\tau a^2 \epsilon_1^3 \left\{ \left( \frac{k_2^2 - k_1^2 - k_3^2}{k_1^2} + \frac{k_1^2 - k_2^2 - k_3^2}{k_2^2} \right) \zeta_{k_1}^{\prime*}(\tau) \zeta_{k_2}^{\prime*}(\tau) \zeta_{k_3}^*(\tau) + \text{perm} \right\} \right], \quad (\text{A6})$$

$$B_\zeta^6(k_1, k_2, k_3) = -\frac{1}{2} \text{Im} \left[ \zeta_{k_1}(\tau_*) \zeta_{k_2}(\tau_*) \zeta_{k_3}(\tau_*) \int_{\tau_i}^{\tau_*} d\tau a^2 \epsilon_1^3 \left\{ \frac{k_3^2(k_3^2 - k_1^2 - k_2^2)}{k_1^2 k_2^2} \zeta_{k_1}^{\prime*}(\tau) \zeta_{k_2}^{\prime*}(\tau) \zeta_{k_3}^*(\tau) + \text{perm} \right\} \right], \quad (\text{A7})$$

$$B_\zeta^7(k_1, k_2, k_3) = 2\text{Im} \left[ \zeta_{k_1}(\tau_*) \zeta_{k_2}(\tau_*) \zeta_{k_3}(\tau_*) (a^2 \epsilon_1 \eta \zeta_{k_1}^*(\tau) \zeta_{k_2}^*(\tau) \zeta_{k_3}^{\prime*}(\tau) + \text{perm}) \right]_{\tau_i}^{\tau_*}, \quad (\text{A8})$$

$$B_\zeta^8(k_1, k_2, k_3) = 2\text{Im} \left[ \zeta_{k_1}(\tau_*) \zeta_{k_2}(\tau_*) \zeta_{k_3}(\tau_*) \times \left( \frac{a}{H} \zeta_{k_1}^*(\tau) \zeta_{k_2}^*(\tau) \zeta_{k_3}^*(\tau) \right) \times \left\{ 54(aH)^2 + 2(1 - \epsilon_1)(\mathbf{k}_1 \cdot \mathbf{k}_2 + \text{perm}) + \frac{1}{2(aH)^2} [(\mathbf{k}_1 \cdot \mathbf{k}_2) k_3^2 + \text{perm}] \right\} \right]_{\tau_i}^{\tau_*}, \quad (\text{A9})$$

$$B_\zeta^9(k_1, k_2, k_3) = -\text{Im} \left[ \zeta_{k_1}(\tau_*) \zeta_{k_2}(\tau_*) \zeta_{k_3}(\tau_*) \left\{ \frac{\epsilon_1}{H^2} \zeta_{k_1}^*(\tau) \zeta_{k_2}^*(\tau) \zeta_{k_3}^{\prime*}(\tau) \times \left[ k_1^2 + k_2^2 - \left( \frac{\mathbf{k}_1 \cdot \mathbf{k}_3}{k_3} \right)^2 - \left( \frac{\mathbf{k}_2 \cdot \mathbf{k}_3}{k_3} \right)^2 \right] + \text{perm} \right\} \right]_{\tau_i}^{\tau_*}, \quad (\text{A10})$$

$$B_\zeta^{10}(k_1, k_2, k_3) = 2\text{Im} \left[ \zeta_{k_1}(\tau_*) \zeta_{k_2}(\tau_*) \zeta_{k_3}(\tau_*) \left\{ \frac{a\epsilon_1}{H} \zeta_{k_1}^*(\tau) \zeta_{k_2}^{\prime*}(\tau) \zeta_{k_3}^{\prime*}(\tau) \left[ 2 - \epsilon_1 + \epsilon_1 \left( \frac{\mathbf{k}_2 \cdot \mathbf{k}_3}{k_2 k_3} \right)^2 \right] + \text{perm} \right\} \right]_{\tau_i}^{\tau_*}, \quad (\text{A11})$$

where

$$\eta = \dot{\epsilon}_1/H\epsilon_1,$$

$\tau_i$  is the early time when all relevant modes are well within the horizon and the plane-wave initial condition is imposed.  $\tau_*$  is the late time when all relevant modes have been frozen.

- 
- [1] B. J. Carr and S. W. Hawking, *Mon. Not. R. Astron. Soc.* **168**, 399 (1974).
- [2] S. Hawking, *Mon. Not. R. Astron. Soc.* **152**, 75 (1971).
- [3] P. Ivanov, P. Naselsky, and I. Novikov, *Phys. Rev. D* **50**, 7173 (1994).
- [4] P. H. Frampton, M. Kawasaki, F. Takahashi, and T. T. Yanagida, *J. Cosmol. Astropart. Phys.* **04** (2010) 023.
- [5] K. M. Belotsky, A. D. Dmitriev, E. A. Esipova, V. A. Gani, A. V. Grobov, M. Y. Khlopov, A. A. Kirillov, S. G. Rubin, and I. V. Svadkovsky, *Mod. Phys. Lett. A* **29**, 1440005 (2014).
- [6] M. Y. Khlopov, S. G. Rubin, and A. S. Sakharov, *Astropart. Phys.* **23**, 265 (2005).
- [7] S. Clesse and J. García-Bellido, *Phys. Rev. D* **92**, 023524 (2015).
- [8] B. Carr, F. Kuhnel, and M. Sandstad, *Phys. Rev. D* **94**, 083504 (2016).
- [9] K. Inomata, M. Kawasaki, K. Mukaida, Y. Tada, and T. T. Yanagida, *Phys. Rev. D* **96**, 043504 (2017).
- [10] J. García-Bellido, *J. Phys. Conf. Ser.* **840**, 012032 (2017).
- [11] E. D. Kovetz, *Phys. Rev. Lett.* **119**, 131301 (2017).
- [12] B. P. Abbott *et al.* (LIGO Scientific and Virgo Collaborations), *Phys. Rev. Lett.* **116**, 061102 (2016).
- [13] B. P. Abbott *et al.* (LIGO Scientific and Virgo Collaborations), *Phys. Rev. Lett.* **116**, 241103 (2016).
- [14] S. Bird, I. Cholis, J. B. Muñoz, Y. Ali-Haïmoud, M. Kamionkowski, E. D. Kovetz, A. Raccanelli, and A. G. Riess, *Phys. Rev. Lett.* **116**, 201301 (2016).
- [15] M. Sasaki, T. Suyama, T. Tanaka, and S. Yokoyama, *Phys. Rev. Lett.* **117**, 061101 (2016); **121**, 059901(E) (2018).
- [16] G. Sato-Polito, E. D. Kovetz, and M. Kamionkowski, *Phys. Rev. D* **100**, 063521 (2019).
- [17] Y. Akrami *et al.* (Planck Collaboration), *Astron. Astrophys.* **641**, A10 (2020).
- [18] C. Germani and T. Prokopec, *Phys. Dark Universe* **18**, 6 (2017).
- [19] H. Motohashi and W. Hu, *Phys. Rev. D* **96**, 063503 (2017).
- [20] H. Di and Y. Gong, *J. Cosmol. Astropart. Phys.* **07** (2018) 007.
- [21] L. Wu, Y. Gong, and T. Li, [arXiv:2105.07694](https://arxiv.org/abs/2105.07694).
- [22] K. Inomata, E. McDonough, and W. Hu, [arXiv:2110.14641](https://arxiv.org/abs/2110.14641).
- [23] C. Fu, P. Wu, and H. Yu, *Phys. Rev. D* **100**, 063532 (2019).
- [24] S. Kawai and J. Kim, *Phys. Rev. D* **104**, 083545 (2021).
- [25] P. Chen, S. Koh, and G. Tumurtushaa, [arXiv:2107.08638](https://arxiv.org/abs/2107.08638).
- [26] Z. Teimoori, K. Rezazadeh, M. A. Rasheed, and K. Karami, *J. Cosmol. Astropart. Phys.* **10** (2021) 018.
- [27] L.-H. Liu and W.-L. Xu, [arXiv:2107.07310](https://arxiv.org/abs/2107.07310).
- [28] R. Zheng, J. Shi, and T. Qiu, [arXiv:2106.04303](https://arxiv.org/abs/2106.04303).
- [29] S. Heydari and K. Karami, [arXiv:2107.10550](https://arxiv.org/abs/2107.10550).
- [30] S. Heydari and K. Karami, [arXiv:2111.00494](https://arxiv.org/abs/2111.00494).
- [31] R.-G. Cai, C. Chen, and C. Fu, *Phys. Rev. D* **104**, 083537 (2021).
- [32] Q. Wang, Y.-C. Liu, B.-Y. Su, and N. Li, *Phys. Rev. D* **104**, 083546 (2021).
- [33] W. Ahmed, M. Junaid, and U. Zubair, [arXiv:2109.14838](https://arxiv.org/abs/2109.14838).
- [34] M. Sasaki, T. Suyama, T. Tanaka, and S. Yokoyama, *Classical Quantum Gravity* **35**, 063001 (2018).
- [35] S. Passaglia, W. Hu, and H. Motohashi, *Phys. Rev. D* **99**, 043536 (2019).
- [36] J. Lin, Q. Gao, Y. Gong, Y. Lu, C. Zhang, and F. Zhang, *Phys. Rev. D* **101**, 103515 (2020).
- [37] Z. Yi, Y. Gong, B. Wang, and Z.-h. Zhu, *Phys. Rev. D* **103**, 063535 (2021).
- [38] Z. Yi, Q. Gao, Y. Gong, and Z.-h. Zhu, *Phys. Rev. D* **103**, 063534 (2021).
- [39] Q. Gao, Y. Gong, and Z. Yi, *Nucl. Phys.* **B969**, 115480 (2021).
- [40] Z. Yi and Z.-H. Zhu, [arXiv:2105.01943](https://arxiv.org/abs/2105.01943).
- [41] F. Zhang, Y. Gong, J. Lin, Y. Lu, and Z. Yi, *J. Cosmol. Astropart. Phys.* **04** (2021) 045.
- [42] F. Zhang, J. Lin, and Y. Lu, *Phys. Rev. D* **104**, 063515 (2021); **104**, 129902(E) (2021).
- [43] M. Solbi and K. Karami, *J. Cosmol. Astropart. Phys.* **08** (2021) 056.
- [44] D. I. Kaiser, *Phys. Rev. D* **52**, 4295 (1995).
- [45] F. L. Bezrukov and M. Shaposhnikov, *Phys. Lett. B* **659**, 703 (2008).
- [46] C. Germani and A. Kehagias, *Phys. Rev. Lett.* **105**, 011302 (2010).
- [47] C. Germani, Y. Watanabe, and N. Wintergerst, *J. Cosmol. Astropart. Phys.* **12** (2014) 009.
- [48] Y. Hamada, H. Kawai, K.-y. Oda, and S. C. Park, *Phys. Rev. Lett.* **112**, 241301 (2014).
- [49] N. Yang, Q. Fei, Q. Gao, and Y. Gong, *Classical Quantum Gravity* **33**, 205001 (2016).
- [50] J. Fumagalli, S. Mooij, and M. Postma, *J. High Energy Phys.* **03** (2018) 038.
- [51] J. Fumagalli, M. Postma, and M. Van Den Bout, *J. High Energy Phys.* **09** (2020) 114.
- [52] J. M. Ezquiaga, J. Garcia-Bellido, and E. Ruiz Morales, *Phys. Lett. B* **776**, 345 (2018).
- [53] F. Bezrukov, M. Pauly, and J. Rubio, *J. Cosmol. Astropart. Phys.* **02** (2018) 040.

- [54] S. Matarrese, S. Mollerach, and M. Bruni, *Phys. Rev. D* **58**, 043504 (1998).
- [55] S. Mollerach, D. Harari, and S. Matarrese, *Phys. Rev. D* **69**, 063002 (2004).
- [56] K. N. Ananda, C. Clarkson, and D. Wands, *Phys. Rev. D* **75**, 123518 (2007).
- [57] D. Baumann, P. J. Steinhardt, K. Takahashi, and K. Ichiki, *Phys. Rev. D* **76**, 084019 (2007).
- [58] J. Garcia-Bellido, M. Peloso, and C. Unal, *J. Cosmol. Astropart. Phys.* **09** (2017) 013.
- [59] R. Saito and J. Yokoyama, *Phys. Rev. Lett.* **102**, 161101 (2009); **107**, 069901(E) (2011).
- [60] R. Saito and J. Yokoyama, *Prog. Theor. Phys.* **123**, 867 (2010); **126**, 351(E) (2011).
- [61] E. Bugaev and P. Klimai, *Phys. Rev. D* **81**, 023517 (2010).
- [62] E. Bugaev and P. Klimai, *Phys. Rev. D* **83**, 083521 (2011).
- [63] L. Alabidi, K. Kohri, M. Sasaki, and Y. Sendouda, *J. Cosmol. Astropart. Phys.* **09** (2012) 017.
- [64] N. Orlofsky, A. Pierce, and J. D. Wells, *Phys. Rev. D* **95**, 063518 (2017).
- [65] T. Nakama, J. Silk, and M. Kamionkowski, *Phys. Rev. D* **95**, 043511 (2017).
- [66] K. Inomata, M. Kawasaki, K. Mukaida, Y. Tada, and T. T. Yanagida, *Phys. Rev. D* **95**, 123510 (2017).
- [67] S.-L. Cheng, W. Lee, and K.-W. Ng, *J. Cosmol. Astropart. Phys.* **07** (2018) 001.
- [68] R.-G. Cai, S. Pi, S.-J. Wang, and X.-Y. Yang, *J. Cosmol. Astropart. Phys.* **05** (2019) 013.
- [69] R.-G. Cai, Z.-K. Guo, J. Liu, L. Liu, and X.-Y. Yang, *J. Cosmol. Astropart. Phys.* **06** (2020) 013.
- [70] R.-G. Cai, S. Pi, S.-J. Wang, and X.-Y. Yang, *J. Cosmol. Astropart. Phys.* **10** (2019) 059.
- [71] G. Domènech, *Universe* **7**, 398 (2021).
- [72] R. D. Ferdman *et al.*, *Classical Quantum Gravity* **27**, 084014 (2010).
- [73] G. Hobbs *et al.*, *Classical Quantum Gravity* **27**, 084013 (2010).
- [74] M. A. McLaughlin, *Classical Quantum Gravity* **30**, 224008 (2013).
- [75] G. Hobbs, *Classical Quantum Gravity* **30**, 224007 (2013).
- [76] P. Amaro-Seoane *et al.* (LISA Collaboration), arXiv:1702.00786.
- [77] W.-R. Hu and Y.-L. Wu, *Natl. Sci. Rev.* **4**, 685 (2017).
- [78] J. Luo *et al.* (TianQin Collaboration), *Classical Quantum Gravity* **33**, 035010 (2016).
- [79] C. Brans and R. H. Dicke, *Phys. Rev.* **124**, 925 (1961).
- [80] P. A. R. Ade *et al.* (BICEP and Keck Collaborations), *Phys. Rev. Lett.* **127**, 151301 (2021).
- [81] D. J. Fixsen, E. S. Cheng, J. M. Gales, J. C. Mather, R. A. Shafer, and E. L. Wright, *Astrophys. J.* **473**, 576 (1996).
- [82] K. Inomata, M. Kawasaki, and Y. Tada, *Phys. Rev. D* **94**, 043527 (2016).
- [83] K. Inomata and T. Nakama, *Phys. Rev. D* **99**, 043511 (2019).
- [84] Y. Ali-Haïmoud, E. D. Kovetz, and M. Kamionkowski, *Phys. Rev. D* **96**, 123523 (2017).
- [85] P. W. Graham, S. Rajendran, and J. Varela, *Phys. Rev. D* **92**, 063007 (2015).
- [86] Y. Lu, A. Ali, Y. Gong, J. Lin, and F. Zhang, *Phys. Rev. D* **102**, 083503 (2020).
- [87] K. Kohri and T. Terada, *Phys. Rev. D* **97**, 123532 (2018).
- [88] J. R. Espinosa, D. Racco, and A. Riotto, *J. Cosmol. Astropart. Phys.* **09** (2018) 012.
- [89] Y. Lu, Y. Gong, Z. Yi, and F. Zhang, *J. Cosmol. Astropart. Phys.* **12** (2019) 031.
- [90] J.-C. Hwang, D. Jeong, and H. Noh, *Astrophys. J.* **842**, 46 (2017).
- [91] K. Tomikawa and T. Kobayashi, *Phys. Rev. D* **101**, 083529 (2020).
- [92] A. Ali, Y. Gong, and Y. Lu, *Phys. Rev. D* **103**, 043516 (2021).
- [93] V. De Luca, G. Franciolini, A. Kehagias, and A. Riotto, *J. Cosmol. Astropart. Phys.* **03** (2020) 014.
- [94] K. Inomata and T. Terada, *Phys. Rev. D* **101**, 023523 (2020).
- [95] C. Yuan, Z.-C. Chen, and Q.-G. Huang, *Phys. Rev. D* **101**, 063018 (2020).
- [96] G. Domènech and M. Sasaki, *Phys. Rev. D* **103**, 063531 (2021).
- [97] Z. Chang, S. Wang, and Q.-H. Zhu, arXiv:2009.11994.
- [98] R.-G. Cai, X.-Y. Yang, and L. Zhao, arXiv:2109.06865.
- [99] B. J. Carr, *Astrophys. J.* **201**, 1 (1975).
- [100] N. Aghanim *et al.* (Planck Collaboration), *Astron. Astrophys.* **641**, A6 (2020); **652**, C4(E) (2021).
- [101] O. Özsoy, S. Parameswaran, G. Tasinato, and I. Zavala, *J. Cosmol. Astropart. Phys.* **07** (2018) 005.
- [102] Y. Tada and S. Yokoyama, *Phys. Rev. D* **100**, 023537 (2019).
- [103] I. Musco and J. C. Miller, *Classical Quantum Gravity* **30**, 145009 (2013).
- [104] T. Harada, C.-M. Yoo, and K. Kohri, *Phys. Rev. D* **88**, 084051 (2013); **89**, 029903(E) (2014).
- [105] A. Escrivà, C. Germani, and R. K. Sheth, *Phys. Rev. D* **101**, 044022 (2020).
- [106] C.-M. Yoo, T. Harada, and H. Okawa, *Phys. Rev. D* **102**, 043526 (2020).
- [107] V. De Luca, G. Franciolini, and A. Riotto, *Phys. Rev. Lett.* **126**, 041303 (2021).
- [108] K. Inomata, M. Kawasaki, K. Mukaida, and T. T. Yanagida, *Phys. Rev. Lett.* **126**, 131301 (2021).
- [109] V. Vaskonen and H. Veermäe, *Phys. Rev. Lett.* **126**, 051303 (2021).
- [110] K. Kohri and T. Terada, *Phys. Lett. B* **813**, 136040 (2021).
- [111] G. Domènech and S. Pi, arXiv:2010.03976.
- [112] S. Vagnozzi, *Mon. Not. R. Astron. Soc.* **502**, L11 (2021).
- [113] M. Kawasaki and H. Nakatsuka, *J. Cosmol. Astropart. Phys.* **05** (2021) 023.
- [114] B. J. Carr, K. Kohri, Y. Sendouda, and J. Yokoyama, *Phys. Rev. D* **81**, 104019 (2010).
- [115] R. Laha, *Phys. Rev. Lett.* **123**, 251101 (2019).
- [116] B. Dasgupta, R. Laha, and A. Ray, *Phys. Rev. Lett.* **125**, 101101 (2020).
- [117] H. Niikura *et al.*, *Nat. Astron.* **3**, 524 (2019).
- [118] K. Griest, A. M. Cieplak, and M. J. Lehner, *Phys. Rev. Lett.* **111**, 181302 (2013).
- [119] P. Tisserand *et al.* (EROS-2 Collaboration), *Astron. Astrophys.* **469**, 387 (2007).
- [120] Y. Ali-Haïmoud and M. Kamionkowski, *Phys. Rev. D* **95**, 043534 (2017).

- [121] V. Poulin, P. D. Serpico, F. Calore, S. Clesse, and K. Kohri, *Phys. Rev. D* **96**, 083524 (2017).
- [122] C. J. Moore, R. H. Cole, and C. P. L. Berry, *Classical Quantum Gravity* **32**, 015014 (2015).
- [123] C. T. Byrnes, M. Gerstenlauer, S. Nurmi, G. Tasinato, and D. Wands, *J. Cosmol. Astropart. Phys.* **10** (2010) 004.
- [124] J. M. Maldacena, *J. High Energy Phys.* **05** (2003) 013.
- [125] P. Creminelli and M. Zaldarriaga, *J. Cosmol. Astropart. Phys.* **10** (2004) 006.
- [126] G. Franciolini, A. Kehagias, S. Matarrese, and A. Riotto, *J. Cosmol. Astropart. Phys.* **03** (2018) 016.
- [127] A. Kehagias, I. Musco, and A. Riotto, *J. Cosmol. Astropart. Phys.* **12** (2019) 029.
- [128] V. Atal and C. Germani, *Phys. Dark Universe* **24**, 100275 (2019).
- [129] F. Ricciardi, M. Taoso, and A. Urbano, *J. Cosmol. Astropart. Phys.* **08** (2021) 060.
- [130] R. Saito, J. Yokoyama, and R. Nagata, *J. Cosmol. Astropart. Phys.* **06** (2008) 024.
- [131] S. Young, C. T. Byrnes, and M. Sasaki, *J. Cosmol. Astropart. Phys.* **07** (2014) 045.
- [132] L. Verde, L.-M. Wang, A. Heavens, and M. Kamionkowski, *Mon. Not. R. Astron. Soc.* **313**, L141 (2000).
- [133] E. Komatsu and D. N. Spergel, *Phys. Rev. D* **63**, 063002 (2001).
- [134] D. K. Hazra, L. Sriramkumar, and J. Martin, *J. Cosmol. Astropart. Phys.* **05** (2013) 026.
- [135] H. V. Ragavendra, D. Chowdhury, and L. Sriramkumar, *arXiv:2003.01099*.
- [136] F. Arroja and T. Tanaka, *J. Cosmol. Astropart. Phys.* **05** (2011) 005.